Available online at www.sciencedirect.com
SCIENCE DIRECT®
Carbohydrate Research 338 (2003) 1679–1689
CARBOHYDRATE RESEARCH
www.elsevier.com/locate/carres

MM3 Potential energy surfaces of the 2-linked glucosyl trisaccharides α-kojitriose and β-sophorotriose☆

Carlos A. Stortz,* Alberto S. Cerezo

Departamento de Química Orgánica-CIHIDECAR, Facultad de Ciencias Exactas y Naturales, Universidad de Buenos Aires, Ciudad Universitaria, 1428 Buenos Aires, Argentina

Received 29 April 2003; accepted 4 June 2003

Abstract

The adiabatic potential energy surfaces (PES) of two trisaccharides with 2-linkages (α-kojitriose and β-sophorotriose) were obtained using the MM3 force field, and are represented by a single 3D contour map for which the energy is plotted against the two ψ glycosidic angles. In spite of the proximity of the positions where the two monosaccharidic units are linked to the central monosaccharide, an almost independent behavior of both linkages was found for the α-linked trisaccharide α-kojitriose, i.e., the surfaces are those expected from the maps of the disaccharide containing the same linkage. A slight shift of the position of the global minimum is found to occur, due to a hydrogen bond between the third and first monosaccharide units, which also leads to an increase in flexibility. On the other hand, for the β-linked trisaccharide β-sophorotriose, the surface is sharply different from that expected by observation of the disaccharide map. Some of the expected minima cannot appear unless a serious deformation of the ϕ and/or ψ angles is produced. Furthermore, the global minimum corresponds to a combination of different conformations for each of the linkages, whereas another minimum with only slightly higher energy has both glycosidic linkages in a conformation less favored for the disaccharide, though close to that predicted in crystal diffraction studies.

Keywords: Trisaccharides; Conformational analysis; Molecular mechanics; MM3; Ramachandran map; Potential energy surfaces; Kojitriose; Sophorotriose

1. Introduction

The significance of oligosaccharide conformations in their functional and biological properties has led to a rising interest in knowing their three-dimensional structures, either by experimental studies or by theoretically based methods. Modeling of disaccharides is usually accompanied by the generation of a Ramachandran-like 3D contour map,[2–5] where the energy is determined for all mutual orientations of the monosaccharide residues expressed by the glycosidic angles ϕ and ψ. Many disaccharides were studied; those representing naturally abundant polysaccharides like amylose or cellulose received the most attention, while those carrying less common linkages, like 1→2, received less consideration. The most representative 2-linked disaccharides, sophorose and kojibiose were studied first by rigid residue analysis,[6–8] and then by flexible residue analysis,[9–12] especially with the appearance of the MM3 force-field,[13,14] which is considered very reliable for carbohydrates. The conformational features of other 2-linked disaccharides (some related to glycoproteins) have also been described in the literature.[15–21] However, in some of the recent studies that incorporated modern techniques (experimental and modeling) for the study of the conformation of disaccharides, those 2-linked were excluded,[22,23] probably due to their scarcity in Nature. A β-(1→2)-linked glucan ('crown gall glucan') has been found in two species of bacteria,[24,25] while α-(1→2)-linked glucose side chains were encountered in a dextran and a teichoic acid also produced by other species of

☆ MM3 Potential energy surfaces of trisaccharides. Part 3. For Part 2, see Ref. 1.

* Corresponding author. Tel./fax: +54-11-45763346.
E-mail address: stortz@qo.fcen.uba.ar (C.A. Stortz).

0008-6215/03/$ - see front matter © 2003 Elsevier Ltd. All rights reserved.
doi:10.1016/S0008-6215(03)00265-9

bacteria.[26,27] A few natural products from plants have oligosaccharidic β-(1→2)-linked glucosyl chains attached to a non-polar moiety.[28,29]

We have recently shown[30] that the ϕ glycosidic angle usually takes a more or less fixed value (at least with MM3). Thus, it can be added to the variables to relax, and a clear correlation is found for the contour maps with the energy related to ϕ and ψ, and to x–y plots with the energy just related to ψ.[30] Therefore, we were able to present the potential energy surfaces (PES) of trisaccharides as contour maps in which the energy is plotted as a function of both ψ glycosidic angles. The method was applied first to cellotriose and maltotriose, indicating no major influence of one linkage over the other.[31] A similar study on the repeating units of carrageenans[1] showed that although in most of the cases each linkage behaves independently, in one case a hydrogen bond between the first and the third monosaccharide units alters the shape of the PES expected from placing both disaccharide maps together. Herein we present a similar application to the 2-linked glucosyl trisaccharides α-kojitriose (α-D-Glc-(1→2)-α-D-Glc-(1→2)-α-D-Glc) and β-sophorotriose (β-D-Glc-(1→2)-β-D-Glc-(1→2)-β-D-Glc). As expected, larger influences of one linkage over the other appear as a result of the contortion originated in the presence of monosaccharide units bound to the contiguous 1- and 2-positions of the central glucose unit.

2. Methods

The molecular mechanics program MM3 (92) (QCPE, Indiana University, USA), developed by Allinger and co-workers, was used,[13,14] but the MM3 routines were modified as suggested[32] by changing the maximum atomic movement from 0.25 to 0.10 Å. A dielectric constant of 4.0 was used throughout the work in order to compare results with published data.[9–11] Minimization was carried out by the block diagonal Newton–Raphson procedure for grid points and using the full-matrix procedure for minima. The dihedrals ϕ and ψ for kojibiose and sophorose are defined† by atoms O-5′–C-1′–O-1′–C-2 and C-1′–O-1′–C-2–C-3, respectively, while ϕ^{H} and ψ^{H} are defined by atoms H-1′–C-1′–O-1′–C-2 and C-1′–O-1′–C-2–H-2, respectively. For kojitriose and sophorotriose, the constitutent monosaccharides are numbered starting from the reducing end. The dihedrals $\phi_{2\rightarrow1}$ and $\psi_{2\rightarrow1}$ are defined† by atoms O-5′–C-1′–O-1′–C-2 and C-1′–O-1′–C-2–C-3, respectively, while $\phi^{H}_{2\rightarrow1}$ and $\psi^{H}_{2\rightarrow1}$ are defined† by atoms H-1′–C-1′–O-1′–C-2 and C-1′–O-1′–C-2–H-2, respectively. The equivalent dihedrals for the 3→2 linkage follow the same conventions, but non-primed atoms should be primed, while those primed should be double-primed.

The orientation of the hydroxyl hydrogen atoms is indicated by χ_n, defined by the atoms H-n–C-n–O-n–H(O)-n, whereas χ_6 is defined by the atoms C-5–C-6–O-6–H(O)-6, and ω by the atoms O-5–C-5–C-6–O-6, singly- or double-primed when necessary. Their values are described by a one-letter code:[33] **S** for angles between −30 and +30°, **g** for 30–80°, **T** for angles with absolute value larger than 150°, and **G** for angles between −30 and −80°. Free energies were calculated as indicated previously.[31,34]

2.1. Generation of disaccharide potential energy surfaces

The general procedure for obtaining 2D plots for describing disaccharides PES has been described elsewhere.[30] The starting orientations of the secondary hydroxyl and hydroxymethyl groups of α-kojibiose and β-sophorose were taken from those yielding at least one grid point in the main ϕ trough reported by Dowd and co-workers[9,10] From these orientations (four for β-sophorose[10] and five for α-kojibiose[9]), low-energy conformers were generated at different values of the ψ angle, varying also the primary hydroxyl torsion angles. These conformers were the starting points for the generation of the PES. For α-kojibiose, 70 different conformers were used, corresponding to 50 unique exocyclic angle orientations, as the process of minimization changed markedly some of the exocyclic angles. For β-sophorose, 24 different minima were utilized, with 16 unique orientations of exocyclic angles. In order to generate the PES, the angle ψ was varied fully using a 10° grid, using the dihedral driver 2 (sequential) for all the conformers, and the dihedral driver 4 (from the initial structure) for each of the unique orientation of exocyclic angles. At each point, energies were calculated after minimization with restraints for these two angles but allowing the other variables (including ϕ) to relax. The optimization was terminated when the decrease in energy converged to a value lower than 2 cal/mol. By recording only the lowest energy value for each ψ angle, an adiabatic PES, or plot of energy as function of the ψ angle was produced.

2.2. Generation of the trisaccharide minima

Different starting orientations of the hydroxyl and hydroxymethyl groups were tested using the conformers that yielded at least one low-energy grid point in the disaccharide maps: for the reducing and non-reducing

† Most of the literature[5,12,18,22,31,33,34] (at least, that related to our work) uses the same definitions for the heavy atoms-referred ϕ and ψ angles, in spite of a different IUPAC-IUB recommendation for the latter angles (ψ defined by atoms C-1′–O-1′–C-x–C-x-1).

ends (monosaccharides 1 and 3), the orientations obtained for the reducing and non-reducing ends of the equivalent disaccharides were used, respectively. For monosaccharide 2, both the orientations occurring at the reducing and non-reducing end of the disaccharide were used. In this way, 48 different combinations of orientations of the exocyclic groups were tested for β-sophorotriose, while 360 different orientations appeared for α-kojitriose. In an automated fashion, unrestrained MM3 full-matrix calculations were carried out for points starting at each of those orientations, at each of the three different combination of the ϕ, ψ angles (in either of both linkages) which gave rise to a minimum in the disaccharide maps. In the final output for each minimum, only those orientations with an energy up to 1 kcal/mol above the lowest in that $\psi_{2\rightarrow1}$,$\psi_{3\rightarrow2}$ region (or higher than that value, but with a very low free energy) were left. The conformers produced were used to generate the maps (see below). During this generation, it was determined that new minima in unexpected regions appeared. These minima were identified, their exocyclic variants were tested, and new starting points for the generation of the map were added. For β-sophorotriose, 77 total conformers were found, corresponding to 45 unique orientations of the exocyclic groups, while for α-kojitriose, 194 different conformers were generated, related to 108 unique orientations of the exocyclic groups.

2.3. Generation of trisaccharide maps

The maps were generated following the general procedures described for di- and trisaccharides.[31,35] As the minimum-energy ϕ angles showed considerable variations in different regions (see below), the MM3 driver 2 (sequential) was used starting from each conformer in four different directions, in order to search as much as possible for low-energy grid points. In such complicated surfaces, the use of this driver in only one direction might have lead to the propagation of inelastic deformations which would have affected[35] the adiabaticity of the maps. Driver 4 was also used, once for each unique orientation of exocyclic angles. In all cases, the angles $\psi_{2\rightarrow1}$ and $\psi_{3\rightarrow2}$ were fully varied using a 20° grid. At each point, energies were calculated after minimization with restraints for these two angles but allowing the other variables (including both ϕ angles) to relax. The optimizations were terminated when the decrease in energy converged to a value lower than 2 cal/mol. The conformational adiabatic maps were produced by recording the lowest energy values for each ψ,ψ combination. In order to recalculate the surface in the region where the main minima appear (both ψ from 165–175° to 290–310°), the starting points that yielded low-energy grid points in this region were submitted to calculations using the same procedure described above, but with a 5° grid. As explained above, the first generation of the maps led to the finding of new minima, which were used as a basis for a new recalculation of the trisaccharide PES.

2.4. Flexibility measurements

The absolute flexibility gives an indication of the ease at which the low-energy conformers overcome barriers to their conformational interconversions. This parameter was calculated for di- and trisaccharides as described previously.[18,31,36] First, the energies and geometries of the transition states between minimum energy regions were calculated: they were first estimated from the walk within the adiabatic maps, and then determined by a full-matrix analysis, confirming that only one negative eigenvalue appeared. When more than one transition state was present in the same region, the one with lower energy was selected. Then, the absolute flexibility Φ was calculated as:

$$\Phi_{p\theta_1} = \sum_{i=1}^{n}\left(\frac{e^{-Ei/RT}}{\sum_{k=1}^{n} e^{-Ei/RT}}\right) \times \left[\sum_{j=1}^{m}(e^{-(Ej-E_{gm})/RT}) \times \left(\frac{\sum_{l=1}^{p}|\theta_{l,i} - \theta_{l,j}|}{p \times 360^{\circ}}\right)\right],$$

where E_{gm} is the energy of the global minimum, n is the number of minima (indexes i and k), m the number of transition states (index j) surrounding minimum i, p is the number of dihedral angles θ been monitored (index l), measured in degrees, R is the universal gas constant, and T the temperature (set to 25 °C = 298.16 K). The above-mentioned formula was also utilized to calculate the absolute flexibilities of the trisaccharides with respect to each glycosidic linkage. For this purpose, the absolute flexibility for each of the paths (when they exist) involving a neat variation of the ψ angle corresponding to this linkage was calculated independently. For each ψ angle all these flexibilities, weighed through their Boltzmann populations were added.

The partition functions were calculated as:[1] $q_{\psi,\psi} = \Delta\psi^2 \times \Sigma_{i=1}^{ES} e^{-(E_i-E_{gm})/RT}$ where $\Delta\psi$ are the grid spacings (20° for full maps, 5° for amplifications) and the summation is carried out over the entire surface determined (e.g., ES = 324 for full maps). French and co-workers[22] used the name 'probability volume' for this function. The partial flexibility on each of the ψ torsional angles of the trisaccharides, was evaluated by generating estimates of the adiabatic [energy vs. $\psi_{3\rightarrow2}$] and [energy vs. $\psi_{2\rightarrow1}$] relationships. These were created by recording the minimum energy in the amplified maps (5° grid) for each column and for each row of data,

respectively. From these data, partial $q_{\psi 3\rightarrow 2}$ and $q_{\psi 2\rightarrow 1}$ values were calculated using the above-mentioned equation, which were extended to the whole ψ range by adding the effect of the remainder of the map (20° grid).

3. Results

The MM3 adiabatic potential energy surfaces for α-kojibiose and β-sophorose, depicted as energy plots related to the glycosidic angle ψ[30] (i.e., with the ϕ angles relaxed to their minimum-energy position in the main trough) are shown on Fig. 1. Table 1 shows the geometrical and energy characteristics of the lower energy minima in each region. α-Kojibiose exhibits a typical three-minima behavior, with a small energy difference (but a substantial potential barrier) between minima **A** and **B**. In the PES of β-sophorose also three minima appear, but the **A** minimum is found in a shallow region.

The MM3 PES of α-kojitriose determined as a contour map relating the energy with both ψ glycosidic angles is shown in Fig. 2, together with the plot obtained by recalculation in the region **A**–**B** of low energy ($\psi_{3\rightarrow 2}$ from 170 to 310°, $\psi_{2\rightarrow 1}$ from 165 to 305°), while the equivalent plots for β-sophorotriose are shown on Fig. 3 (with the expanded region at $\psi_{3\rightarrow 2}$ from 175 to 295°, and $\psi_{2\rightarrow 1}$ from 165 to 290°). The geometrical and energy data on the minima obtained in each region for α-kojitriose are shown in Table 2, while those corresponding to β-sophorotriose are shown in Table 3. The minima are named by a two-letter code according to the minimum energy region (**A**, **B** or **C**) of the 3→2 linkage (first letter) and the 2→1 linkage (second letter).

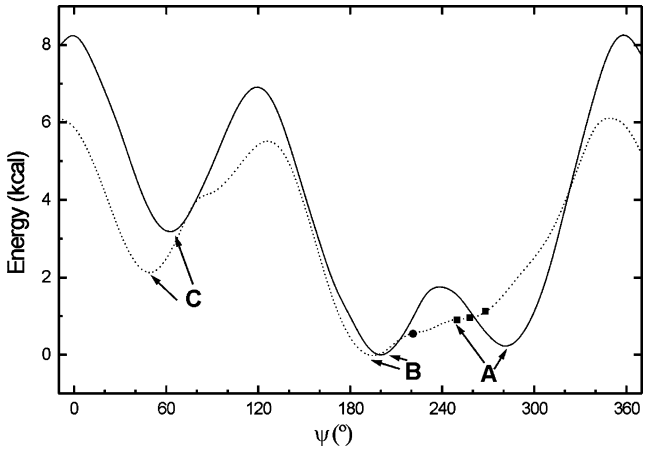

Fig. 1. MM3(92) relaxed surface (2D plot) for α-kojibiose (solid) and β-sophorose (dashed) at $\varepsilon = 4$. Position of the minima is shown in both plots. The symbols show the positions of reported crystal structures for α-sophorose hydrate[37] (●), and several acetylated derivatives of sophorose[38] (■).

Substantial diagonal symmetry (a measurement of the independent behavior of both linkages) is observed in the map of α-kojitriose, but not in that of β-sophorotriose. Table 4 shows the flexibility measurements carried out using the data obtained for the di- and trisaccharides under study. Table 5 shows the main hydrogen bond arrangements established for both di- and trisaccharides in each minimum energy region.

4. Discussion

Most of the earlier flexible-residue molecular modeling studies devoted to disaccharides were oriented to maltose and cellobiose.[2–5] 2-Linked disaccharides, rather uncommon in Nature, have received less attention. Using MM3, Dowd and co-workers obtained the adiabatic conformational surfaces of both anomeric forms of kojibiose and sophorose[9,10] (α- and β-2-linked glucobiose, respectively) at a dielectric constant of 4. The calculations for sophorose were repeated with a different protocol,[11] while further work[12] was made with improved versions of MM3 using different dielectric constants, and with permethylated derivatives.

For α-kojibiose, present calculations (as well as those from Dowd and co-workers[9]) show a typical three-minima pattern (Fig. 1, Table 1), similar to those observed for α-(1→3)-linked galactobioses.[30] Minimum **B** appears only slightly stabilized with respect to **A**, while minimum **C** carries much higher energy. It was determined[12] that lower dielectric constants favor minimum **A** given its hydrogen-bonding possibilities between H(O)-3 and O-5′ (Table 5), while high dielectric constant or permethylation of the hydroxyl groups favor minimum **B**, as the hydrogen bond is weakened or precluded.[12] The relative energy of minimum **C** (stabilized by a hydrogen bond between H(O)-1 and O-5′, Table 5) also follows the same trend. Rigid-residue analysis[8] indicates that **A** is the main minimum. Most of the conformers yielding low energy minima in the adiabatic map carried both hydroxymethyl groups in *GT* orientation, as occurred in previous calculations.[9] Only seldom one of the units carried the *GG* orientation.

For β-sophorose, the map (Fig. 1, Table 1) is also similar to those obtained previously[10–12] with different versions of MM3 and dielectric constants. In the present work, minimum **B** appears as the global one, while the **A** region (1 kcal/mol above) is shallow and wide. It was shown that lower dielectric constants tend to favor minimum **A**, probably because of its possibilities of hydrogen bonding between O-2′ and O-3.[12] However, the permethylated derivative also shows **A** as the global minimum,[12] indicating that other steric factors are concerned. The work by André and co-workers[11] also indicates a shallow **A**–**B** low-energy region, with **A** as the global minimum in an isolated molecule, and a shift

Table 1
Torsion angles (°), relative steric and free energies (kcal/mol) and exocyclic angles for the minimum-energy conformations [a] obtained for α-kojibiose and β-sophorose using the MM3 force-field

	ϕ,ψ	ϕ_H,ψ_H	E_{rel}	G_{rel}	Exocyclic torsion angles [b]			
					$\chi_{2'}\chi_{3'}\chi_{4'}$	$\omega'\chi_{6'}$	$\chi_1\chi_3\chi_4$	$\omega\chi_6$
α-Kojibiose								
A	88, 281	−33, 44	0.21		GgG	gT	ggG	gG
	88, 280	−33, 44		0.86	gGS	gT	ggG	gG
B	83, 200	−37, −41	0.00		TgG	gG	GgG	gG
	87, 200	−33, −40		0.00	gGG	gG	ggG	gG
C	87, 63	−33, 179	3.17		gGG	gT	ggG	gG
	88, 63	−33, 179		4.23	gGS	gT	ggG	gG
TS **A**↔**B**	91, 239	−30, 0	1.75					
β-Sophorose								
A	282, 245	44, 6	1.01	0.25	GgG	gG	ggG	gG
B	271, 193	33, −48	0.00		GgG	gT	GgG	gG
	270, 198	32, −43		0.00	gGS	gT	GgG	gG
C	270, 49	32, 169	2.13	2.83	GgG	gT	ggG	gG
TS **A**↔**B**	Not detected							

Selected data for the main transition states (TS) are also included.
[a] When the steric energy minimum and the free energy minimum structures are not the same, the first line shows the data corresponding to the strain energy minimum, and the second line the data corresponding to the free energy minimum.
[b] For nomenclature, see Section 2.

to the **B** region when a water solution is emulated,[11] in agreement with its weakened hydrogen bonding. In the present calculation, the **A** minimum appears geometrically closer to the **B** region and thus is incapable of engaging in hydrogen bonding between O-2′ and O-3.[39] On the other hand, a weaker hydrogen bond of H(O)-1 with O-5′ and O-6′ appears for minimum **B**, as stated previously.[12] The **C** minimum carries lower energy (Table 1) than that in α-kojibiose, as usually occurs when comparing β- and α-linked disaccharides.[9–12] A crystal structure for the hydrate of α-sophorose[37] exhibits a ψ angle in between the **A** and **B** regions (Fig. 1), while per-O-acetylated derivatives of β-sophorose and its methyl glycoside (not capable of engaging in hydrogen bonds) appear mainly around the **A** region.[38] Experimental NMR measurements in aqueous solution[11] were unable to determine the preferential conformation. In the present map, all of the conformers yielding low energy minima in the adiabatic map carried both hydroxymethyl groups in *GT* orientation, as occurred in previous calculations.[10] Rotamers with one hydroxymethyl in *GG* orientation carry energies at least 0.7 kcal/mol higher. However, solution determinations[11] indicated almost equal proportions of *GT* and *GG* conformers on each unit, while crystal structures reported for sophorose derivatives indicated that most of them carried *GG* orientations.[11]

Partition functions indicate similar glycosidic linkage flexibility for α-kojibiose and β-sophorose (Table 4), intermediate between those of β-cellobiose and α-maltose.[31] Similar results have been found for the tetrahydropyranyl derivatives with the same linkage configurations of these disaccharides.[12] On the other hand, previous work with the actual disaccharides showed sophorose as more flexible than kojibiose.[9,10,12] This would agree with the expected increase in flexibility arising from a diequatorial linkage against an axial–equatorial one.[22,40–42] Determination of absolute flexibility is seriously hindered for β-sophorose, as no pathway (and thus, no transition state) can be found between the **A** and **B** minima. Thus, its low flexibility value arises only from their conformational interconversion to the **C** minimum. The absolute flexibility of α-kojibiose is higher (Table 4), but given the considerable barrier between minima **A** and **B** (Fig. 1, Table 1), is markedly lower than those of cellobiose and maltose.[31]

Conformational analysis of tri- or higher oligosaccharides by modeling was usually carried out by molecular dynamics,[43] by other heuristic procedures,[18] or by taking each glycosidic linkage independently, giving rise to one ϕ, ψ contour map per glycosidic linkage for oligosaccharides with no repeating units.[18,20,43,44] However, the ϕ glycosidic angle was found to take a more or less fixed value for most of the disaccharides, at least using MM3.[30] Even if the 'side-of-the-map' minima[12] may be significant for some equatorially linked disaccharides, their populations are usually negligible[12] at dielectric constants above 1.5. It was previously shown that the ϕ angle could also be allowed to relax, as a clear correlation was found

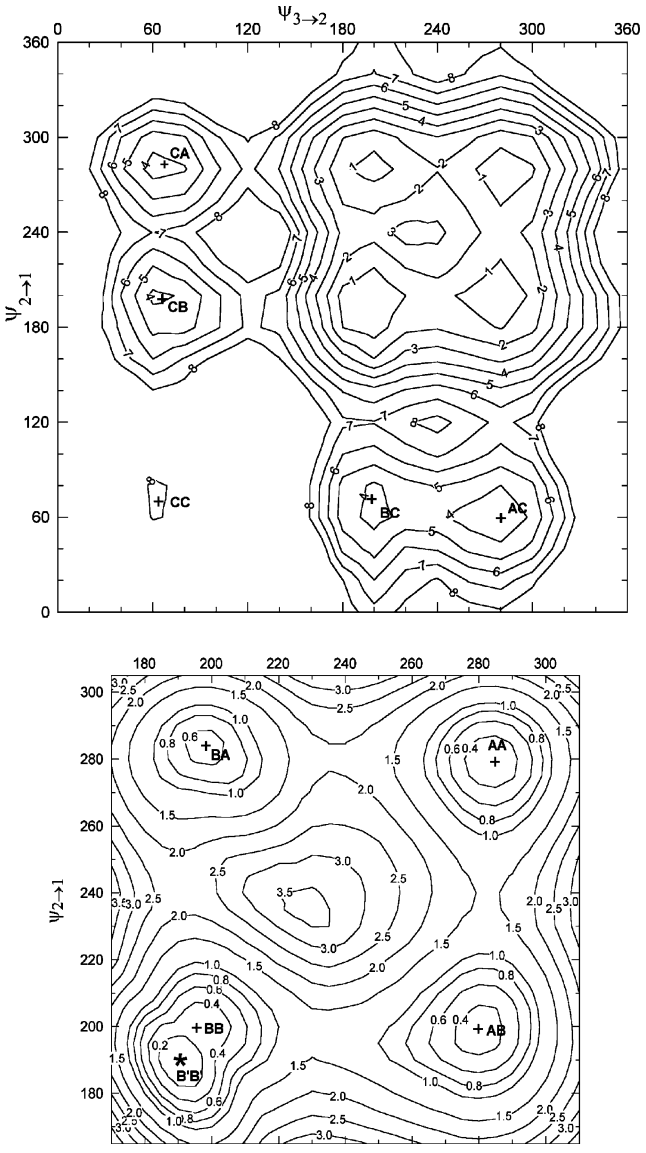

Fig. 2. MM3 (92) adiabatic conformational maps of α-kojitriose (energy vs. $\psi_{3\rightarrow2}$, $\psi_{2\rightarrow1}$) at $\varepsilon = 4$. Above: total map. Iso-energy contour lines are graduated in 1 kcal/mol increments above the global minimum. Below: recalculation in the low energy-region. Iso-energy contour lines are graduated in 0.2 kcal/mol increments above the global minimum, up to 1 kcal/mol. The symbols (+) indicate: (*) MM3 global minima; (+) MM3 local minima.

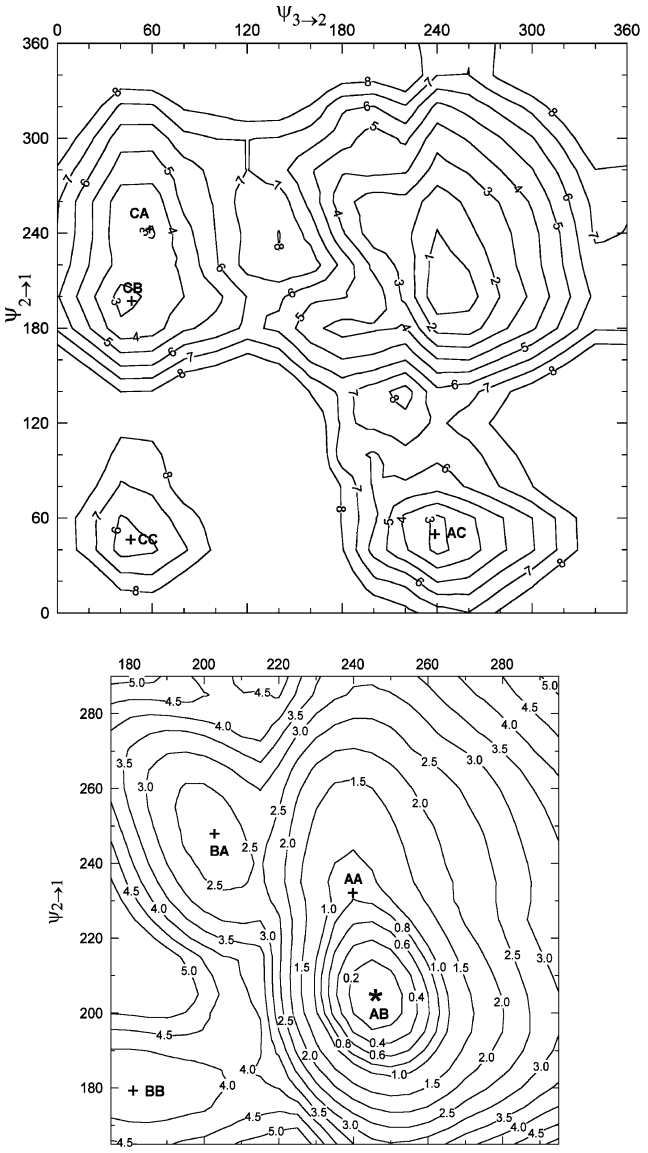

Fig. 3. MM3 (92) adiabatic conformational maps of β-sophorotriose (energy vs. $\psi_{3\rightarrow2}$, $\psi_{2\rightarrow1}$) at $\varepsilon = 4$. Above: total map. Iso-energy contour lines are graduated in 1 kcal/mol increments above the global minimum. Below: recalculation in the low energy-region Iso-energy contour lines are graduated in 0.2 kcal/mol increments above the global minimum, up to 1 kcal/mol. The symbols (+) indicate: (*) MM3 global minima; (+) MM3 local minima.

between the 3D contour maps (energy vs. ϕ and ψ) and the 2D plots (energy vs. ψ).[30] Therefore, it was found that the PES of a trisaccharide might be represented by a contour map, where the energy is plotted against both ψ angles, while the ϕ angles are allowed to relax. The method was applied to the 4-linked glucosyl trisaccharides maltotriose and cellotriose, where both glycosidic linkages behave more or less independently.[31] However, a slight reduction in flexibility was found when passing from the di- to the trisaccharides, especially for the linkage closer to the reducing end.[31] When the method was applied to six different trisaccharide units present in carrageenans (with alternating α-(1→3)- and β-(1→4)-linkages),[1] it was found that five of them show the expected independent behavior (with minor factors altering the additive effect of both linkages), but also that the presence of a sulfate group on C-2 of a β-galactose reducing end produces a new minimum originated in a hydrogen bond between the first and third monosaccharide moieties of the trisaccharide, leading to an unexpected shape of the PES and an increased flexibility.[1] Such inter-unit hydrogen bonds

Table 2
Torsion angles (°), relative steric and free energies (kcal/mol) and exocyclic angles for the minimum-energy conformations obtained for α-kojitriose using the MM3 force-field

	$\phi_{3\to2},\psi_{3\to2}$	(ϕ^H,ψ^H)	$\phi_{2\to1}$, $\psi_{2\to1}$	(ϕ^H,ψ^H)	E_{rel} [a]	Exocyclic torsion angles [b]		
Steric energy minima								
AA	87, 284	−34, 47	89, 279	−32, 43	0.27	TgGgT	gGgT	ggGgG
AB	88, 280	−33, 43	80, 199	−39, −42	0.29	GgGgT	gGgG	ggGgG
AC	87, 278	−34, 40	86, 60	−34, 177	3.09	GgGgT	gGgT	ggGgG
BA	77, 198	−44, −43	87, 284	−32, 47	0.49	TgGgG	gGgT	ggGgG
BB	74, 197	−47, −44	74, 200	−46, −41	0.21	gGSgG	gGgG	ggGgG
BC	71, 197	−50, −44	82, 69	−38, −174	3.34	gGSgG	gGgT	ggGgG
B′B′	76, 191	−44, −51	69, 190	−50, −52	0.00	GgGgG	gGgG	GgGgT
CA	98, 66	−23, 178	87, 282	−33, 45	3.39	gGGgT	gGgT	ggGgG
CB	106, 67	−14, −177	67, 196	−53, −45	3.56	gGGgT	gGgG	ggGgG
CC	110, 65	−9, −179	78, 70	−42, −173	7.44	gGGgT	gGgG	ggGgG
Free energy minima								
AA	88, 283	−33, 46	89, 279	−31, 42	0.98	ggGgT	gGgT	ggGgG
AB	88, 279	−33, 42	80, 197	−39, −43	0.00	gSGgT	gGgG	ggGgG
AC	87, 277	−34, 39	86, 60	−34, 176	4.33	ggGgT	gGgT	ggGgG
BA	82, 200	−38, −41	89, 282	−31, 45	0.59	ggGgG	gGgT	ggGgG
BB	73, 198	−47, −44	74, 200	−46, −41	0.68	gSGgG	gGgG	ggGgG
BC	70, 197	−50, −44	82, 69	−38, −175	4.80	gSGgG	gGgT	ggGgG
B′B′	76, 191	−44, −51	69, 189	−51, −53	1.59	GgGgG	gGgT	GgGgT
CA	same as steric minimum				4.75	gGGgT	gGgT	ggGgG
CB	106, 67	−14, −177	67, 196	−53, −45	5.23	gSGgT	gGgG	ggGgG
CC	same as steric minimum				9.79	gGGgT	gGgG	ggGgG
Main transition states								
AA↔AB	87, 283	−34, 46	92, 239	−27, 0	1.40			
AA↔BA	91, 237	−29, −2	88, 280	−32, 43	1.95			
AB↔BB	92, 229	−28, −11	74, 197	−46, −44	1.32			
BA↔BB	68, 192	−52, −50	88, 241	−31, 1	2.14			

Selected data for the main transition states (TS) are also included.
[a] Steric energy or free energy, depending on the listing.
[b] The angles are given in the order $\chi_{2''}\chi_{3''}\chi_{4''}$ $\omega''\chi_{6''}$ $\chi_{3'}\chi_{4'}$ $\omega'\chi_{6'}$ $\chi_1\chi_3\chi_4$ $\omega\chi_6$. For nomenclature of the angles, see Section 2.

have been already observed experimentally for panose.[45,46]

It might have been expected that (1→2)-linked trisaccharides could have interacting linkages,[31] thus leading to trisaccharide PES quite different from those expected by inspection of the disaccharide PES. However, in the case of the α-linked trisaccharide α-kojitriose, an almost independent behavior of both linkages was found: the three minima appearing for each linkage are transformed into nine minima, with ϕ, ψ angles very close to those encountered for the disaccharide, (Fig. 2, cf. Tables 1 and 2) and relative energies close to those expected from the disaccharide PES. In order to produce minima of each linkage in the **B** region, a slight decrease ($\sim$10–15°) of the ϕ angle occurs, while those carrying the (3→2)-linkage in the **C** region had their corresponding ϕ angles increased ($\sim$10–20°). However, the global minimum was not the expected one in the actual **BB** position, but another one slightly shifted (**B′B′**, Table 2, Fig. 2), where a variation in some of the exocyclic angles gives rise to a strong hydrogen bond between H(O)-2″ and O-1. In **BB** a hydrogen bond between the same oxygens (but the other hydrogen atom) is involved (Table 5). Fig. 4 shows molecular drawings for the minima **BB** and **B′B′**. The presence of this new minimum alters the shape of the individual paths leading from **A** to **B** (Fig. 5), thus increasing the flexibility of each of the linkages in the trisaccharide with respect to that of the disaccharide (Table 4). For the (3→2)-linkage, the increase in flexibility is observed by either flexibility measurement, while for the (2→1)-linkage, only by observing absolute flexibility (Table 4). The PES shows the presence of four minimum-energy wells with energy below 1 kcal (Fig. 2), similar to that observed for β-cellotriose.[31] However, the barriers between those wells are higher for the present trisaccharide (cf the relative energy of the transition states, >1.32 kcal/mol in the present study, <0.55 kcal/mol for β-cellotriose[31]). In any case, the energy differences between the five main minima (Table 2) are not

Table 3
Torsion angles (°), relative steric and free energies (kcal/mol) and exocyclic angles for the minimum-energy conformations [a] obtained for β-sophorotriose using the MM3 force-field

	$\phi_{3\to2},\psi_{3\to2}$	(ϕ^H,ψ^H)	$\phi_{2\to1},\psi_{2\to1}$	(ϕ^H,ψ^H)	E_{rel} [a]	Exocyclic torsion angles [b]		
Steric energy minima								
AA	284, 240	45, 1	280, 232	42, −7	0.81	GgGgG	gGgG	GgGgG
AB	284, 246	46, 8	268, 204	30, −38	0.00	GgGgG	gGgT	GgGgG
AC	283, 239	45, 1	268, 50	29, 170	2.36	GgGgG	gGgT	GgGgG
BA	226, 202	−15, −40	283, 249	44, 11	2.23	GgGgT	gGgG	GSGgG
BB	254, 180	15, −62	273, 180	33, −61	3.59	GgGgG	gGgT	SgGgG
CA	273, 54	35, 173	287, 242	47, 4	2.85	GgGgT	gGgG	GgGgG
CB	270, 46	32, 166	267, 194	28, −47	2.45	GgGgT	gGgT	GgGgG
CC	276, 46	38, 165	276, 46	38, 165	5.29	GgGgT	gGgT	ggGgG
Free energy minima								
AA	same as steric minimum				0.62	GgGgG	gGgG	GgGgG
AB	281, 249	43, 11	268, 205	30, −37	0.00	GgGgT	GGgT	GgGgG
AC	same as steric minimum				3.05	GgGgG	gGgT	GgGgG
BA	225, 211	−16, −29	284, 240	45, 2	1.77	GgGgT	GSgG	GSGgG
BB	255, 183	16, −59	273, 180	33, −61	3.52	GgGgT	gGgT	SgGgG
CA	273, 51	35, 170	287, 240	47, 1	2.94	SgGgT	gGgG	GgGgG
CB	same as steric minimum				2.96	GgGgT	gGgT	GgGgG
CC	278, 49	40, 168	276, 47	37, 167	6.27	gSGgT	gGgT	GgGgG
Main transition states								
AB↔BB	227, 208	−14, −33	272, 183	33, −58	4.04			
AB↔AC	284, 243	45, 4	281, 125	43, −118	6.79			
BA↔CA	293, 106	56, −137	293, 292	54, 55	6.75			
BB↔CB	281, 129	43, −115	271, 189	30, −52	5.98			

Selected data for the main transition states (TS) are also included.
[a] Steric energy or free energy, depending on the listing.
[b] The angles are given in the order $\chi_{2''}\chi_{3''}\chi_{4''}\ \omega''\chi_{6''}\chi_{3'}\chi_{4'}\ \omega'\chi_{6'}\ \chi_1\chi_3\chi_4\ \omega\chi_6$. For nomenclature of the angles, see Section 2.

significant. As expected from the hydrogen bonds present in the disaccharide, minima in the **A** region for the (3→2)-linkage are stabilized by hydrogen bonds between H(O)-3′ and O-5″, while those in the same region for the (2→1)-linkage carry hydrogen bonds between H(O)-3 and O-5′ (Table 5). When the (3→2)-linkage is in the **C** region, a hydrogen bond between H(O)-3′ and O-2″ appears (not observed in the disaccharide, probably because of a different ϕ angle), while when a minimum in the same region is observed for the (2→1)-linkage, the expected H(O)-1–O-5′ bond appears (Table 5). Besides the mentioned hydrogen bonds between the first and third monosaccharide residues in **BB** and **B′B′** (Fig. 4, Table 5), other less important minima (**BC**, **CB** and **CC**) also exhibit different long-range hydrogen bonds (Table 5). A rigid-residue analysis for an α-(1→2)-glucan indicates that, if a regular repeating conformation is adopted, it will correspond to **AA**, where strong cooperative hydrogen bonds between O-3 and O-5′ are encoun-

Table 4
Corrected partition functions q and absolute flexibilities Φ calculated for the compounds under study

		q_ψ (°)		$\Phi_{\phi,\psi}$ ($\times 10^4$)	Φ_ψ ($\times 10^4$)	$\Phi_{\phi,\psi}/\Phi_\psi$
α-Kojibiose		49		33	58	0.57
β-Sophorose		48		0.18	0.32	0.56
	$q_{\psi,\psi}$ (°^{2})	q_ψ (°)	$\Phi_{\phi,\psi,\phi,\psi}$ ($\times 10^4$)	$\Phi_{\psi,\psi}$ ($\times 10^4$)	Φ_ψ ($\times 10^4$)	$\Phi_{\phi,\psi,\phi,\psi}/\Phi_{\psi,\psi}$
α-Kojitriose	2727	$q_{\psi3\to2}=51$ [a] $q_{\psi2\to1}=44$ [a]	57	88	$\Phi_{\psi3\to2}=105$ $\Phi_{\psi2\to1}=95$	0.65
β-Sophorotriose	1008	$q_{\psi3\to2}=<26$ [a] $q_{\psi2\to1}=37$ [a]	0.69	0.68	$\Phi_{\psi3\to2}=0.88$ $\Phi_{\psi2\to1}=0.02$	1.01

[a] Estimated from the 3D map (see Section 2).

Table 5
Hydrogen bond arrangements (with $E_{HB} > 0.3$ kcal/mol) established for every MM3 minimum of kojitriose and sophorotriose, as well as their equivalent disaccharides

Hydrogen bond	Minima
α-Kojibiose	
H(O)-3–O-5′	**A**
H(O)-1–O-5′	**C**
β-Sophorose	
H(O)-3–O-5′	**C**
H(O)-1–O-5′	**B**
H(O)-1–O-6′	**B**
α-Kojitriose	
On contiguous monosaccharide units	
H(O)-3′–O-5″	**AA, AB, AC**
H(O)-3′–O-2″	**CA, CB, CC**
H(O)-3–O-5′	**AA, BA, CA**
H(O)-1–O-5′	**AC, BC, CC**
Between the first and third monosaccharide units	
H(O)-1–O-2″	**BB**
H(O)-2″–O-1	**B′B′**
H(O)-1–O-5″	**CB**
H(O)-3–O-2″	**BC**
H(O)-3–O-5″	**CC**
β-Sophorotriose	
On contiguous monosaccharide units	
H(O)-3′–O-5″	**CA, CB, CC**
H(O)-3–O-5′	**AC, CC**
H(O)-1–O-5′	**AA, AB, CA, CB**
H(O)-1–O-6′	**BB, CB**
H(O)-2″–O-3′	variants of **BA**
Between the first and third monosaccharide units	
H(O)-2″–O-1	**CC**
H(O)-3–O-2″	**CA**
H(O)-3–O-6″	**BA**
H(O)-2″–O-1	**CC**
H(O)-3–O-5″	**AB**

tered.[8] All of the minima obtained using steric or free energy measurements carry all their hydroxymethyl groups in *GT* orientation (Table 2).

A different picture is observed when passing from β-sophorose to β-sophorotriose. For the region where the (3→2)-linkage is in the **A** region, the path for the (2→1)-linkage is very similar to that observed in the disaccharide, with **AB** as the global minimum, **AA** in a shallow region and an energy about 1 kcal/mol higher, and **AC** with an energy about 3 kcal/mol above that of the global minimum (Table 3, Fig. 3). The flexibility observed for this path of the trisaccharide is further reduced with respect to that of the disaccharide (Table 4). However, the geometry of the trisaccharide hinders the presence of a glycosidic angle ψ in the region **B** for the (3→2)-linkage: while minimum **B** is the global minimum for the disaccharide, no minimum appears in an equivalent **BB** region. There is a **BB**-like minimum, but carrying a marked difference in ϕ and especially in ψ values (cf Tables 1 and 3, Fig. 3). Furthermore, this minimum carries high energy, 3.6 kcal/mol above that of the global minimum (**AB**). The minimum **BA** also appears with high energy (2.2 kcal/mol, similar to that of **AC**), but in this case the (3→2)-linkage suffers from a serious deformation in the ϕ angle, which is beyond the value predicted by the exo-anomeric effect (Fig. 6). This structure is stabilized by a long-range hydrogen bond between H(O)-3 and O-6″ (Table 5, Fig. 6). Furthermore, the deformation in the ϕ angle leads to some extent of hydrogen bonding between H(O)-2″ and O-3′, expected to appear (but not found) for the disaccharide,[39] and appearing in some conformers in the **BA** region. The shape of the map is similar to that of α-maltotriose,[31] with one main minimum, and other, less important, secondary minima. Rigid-residue studies for β-(1→2)-linked glucans indicate that, if a regular structure exists, it should carry minima in the **A** region,[7] probably stabilized by hydrogen bonds between O-2′ and O-3. Crystal structures for disaccharide derivatives also encounter its conformation around the **A** region,[38] or in between regions **A** and **B**.[37] The hydrogen bond

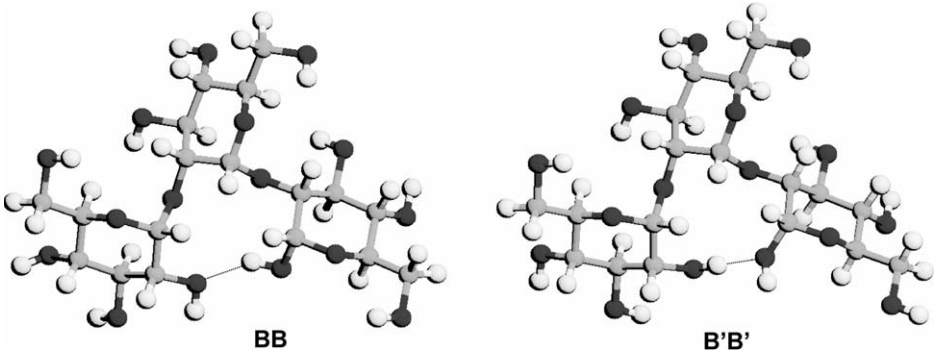

Fig. 4. Drawing of the minimum energy conformers **BB** and **B′B′** of α-kojitriose, showing the hydrogen bonds between the first and third residues.

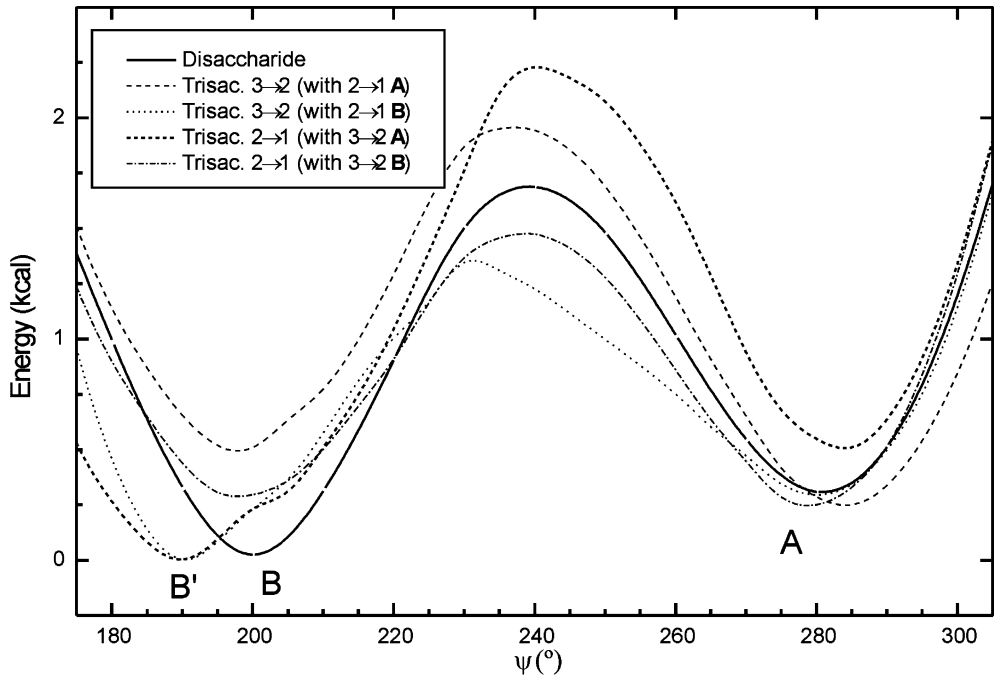

Fig. 5. 2D representations of the paths involving interconversion of the **A** and **B** minima in α-kojibiose and α-kojitriose. Correspondence of line styles and paths is shown on the legend.

present in the disaccharide between H(O)-3 and O-5′ for minima in the **C** region also appears in the trisaccharides within the same region of either linkage (Table 5). In the disaccharide there were also hydrogen bonds linking H(O)-1 with O-5′ and O-6′ for minimum **B**. The latter bond appears for minima **BB** and **CB**, as expected, while the former appears not only for the expected **AB** and **CB**, but also for **AA** and **CA** (Table 5). Long-range hydrogen bonds are produced involving different atoms (Table 5). As mentioned previously, in **BA** there is a link between H(O)-3 with O-6″. In the global minimum **AB**, the same hydrogen atom is bonded to O-5″ (Fig. 6). All of the minima obtained using steric or free energy measurements carry all their hydroxymethyl groups in *GT* orientation (Table 3), even though experimental measurements in solution or crystalline state indicated an important proportion of *GG* rotamers[11] (see above)

This work shows again the advantages of mapping trisaccharides by the way of 3D contours in comparison with those of the single disaccharides. The information on the conformations and their interconversions is harder to view without the picture, and these studies are aided by flexibility measurements. Further studies on 2-linked mannosyl trisaccharides may help to throw more light on these subjects, as the axial O-2 in mannose may change substantially the extrapolation. Furthermore, Rees and Scott have predicted that an α-(1→2)-mannan will not show the crumpled conformation

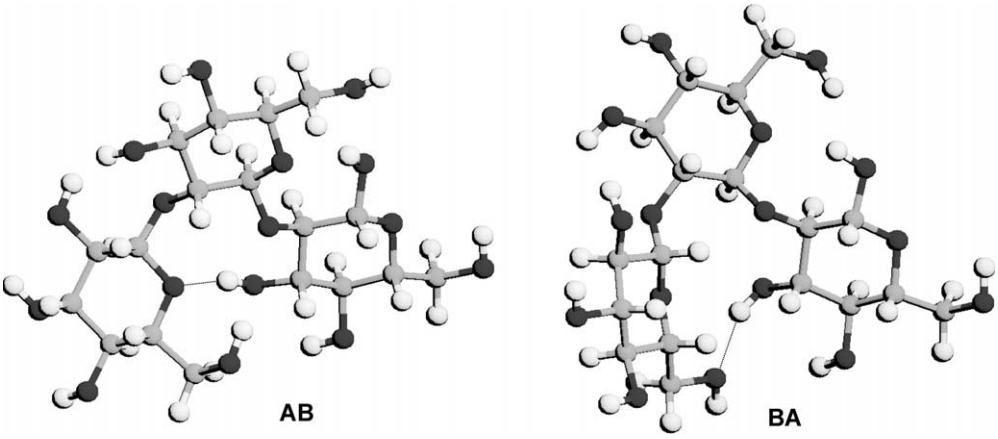

Fig. 6. Drawing of the minimum energy conformers **AB** and **BA** of β-sophorotriose, showing the hydrogen bonds between the first and third residues.

expected in other 2-linked galactans, glucans or β-mannan.[6]

Acknowledgements

Both authors are Research Members of the National Research Council of Argentina (CONICET). This work was supported by a grant from UBA (X-087). The help of Dr E. Jares with the search of crystal structures is also acknowledged.

References

1. Stortz, C.A.; Cerezo, A.S. *Biopolymers*, in press.
2. French, A. D.; Brady, J. W. *ACS Symp. Ser.* **1990**, *430*, 1–19.
3. Engelsen, S. B.; Rasmussen, K. *Int. J. Biol. Macromol.* **1993**, *15*, 56–62.
4. French, A. D.; Dowd, M. K. *J. Mol. Struct. (Theochem)* **1993**, *286*, 183–201.
5. Tran, V.; Buléon, A.; Imberty, A.; Pérez, S. *Biopolymers* **1989**, *28*, 679–690.
6. Rees, D. A.; Scott, W. E. *J. Chem. Soc. Sect. B* **1971**, 469–479.
7. Sathyanarayana, B. K.; Rao, V. S. R. *Biopolymers* **1971**, *10*, 1605–1615.
8. Sathyanarayana, B. K.; Rao, V. S. R. *Biopolymers* **1972**, *11*, 1379–1394.
9. Dowd, M. K.; Zeng, J.; French, A. D.; Reilly, P. J. *Carbohydr. Res.* **1992**, *230*, 223–244.
10. Dowd, M. K.; French, A. D.; Reilly, P. J. *Carbohydr. Res.* **1992**, *233*, 15–34.
11. André, I.; Mazeau, K.; Taravel, F. R.; Tvaroska, I. *New J. Chem.* **1995**, *19*, 331–339.
12. Mendonca, S.; Johnson, G. P.; French, A. D.; Laine, R. A. *J. Phys. Chem. A* **2002**, *106*, 4115–4124.
13. Allinger, N. L.; Yuh, Y. H.; Lii, J.-H. *J. Am. Chem. Soc.* **1989**, *111*, 8551–8566.
14. Allinger, N. L.; Rahman, M.; Lii, J.-H. *J. Am. Chem. Soc.* **1990**, *112*, 8293–8307.
15. Imberty, A.; Gerber, S.; Tran, V.; Pérez, S. *Glycoconjugate J.* **1990**, *7*, 27–54.
16. Peters, T. *Liebigs Ann. Chem.* **1991**, 135–141.
17. Stevens, E. S. *Biopolymers* **1994**, *34*, 1403–1407.
18. Koča, J.; Pérez, S.; Imberty, A. *J. Comput. Chem.* **1995**, *16*, 296–310.
19. Dowd, M. K.; French, A. D.; Reilly, P. J. *J. Carbohydr. Chem.* **1995**, *14*, 589–600.
20. Mazeau, K.; Pérez, S. *Carbohydr. Res.* **1998**, *311*, 203–217.
21. Khatuntseva, E. A.; Ustuzhanina, N. E.; Zatonskii, G. V.; Shashkov, A. S.; Usov, A. I.; Nifant'ev, N. E. *J. Carbohydr. Chem.* **2000**, *19*, 1151–1173.
22. French, A. D.; Kelterer, A.-M.; Johnson, G. P.; Dowd, M. K.; Cramer, C. J. *J. Comput. Chem.* **2001**, *22*, 65–78.
23. Cheetham, N. W. H.; Dasgupta, P.; Ball, G. E. *Carbohydr. Res.* **2003**, *338*, 955–962.
24. Putman, E. W.; Potter, A. L.; Hodgson, R.; Hassid, W. Z. *J. Am. Chem. Soc.* **1950**, *72*, 5024–5026.
25. Dedonder, R. A.; Hassid, W. Z. *Biochim. Biophys. Acta* **1964**, *90*, 239–248.
26. Usui, T.; Kobayashi, M.; Yamaoka, N.; Matsuda, K.; Tuzimura, K. *Tetrahedron Lett.* **1973**, *36*, 3397–3400.
27. Wicken, A. J.; Baddiley, J. *Biochem. J.* **1963**, *87*, 54–62.
28. Brinkmeier, E.; Geiger, H.; Zinsmeister, H. D. *Phytochemistry* **1999**, *52*, 297–302.
29. Schmid, R. D.; Harborne, J. B. *Phytochemistry* **1973**, *12*, 2269–2273.
30. Stortz, C. A.; Cerezo, A. S. *Carbohydr. Res.* **2002**, *337*, 1861–1871.
31. Stortz, C. A.; Cerezo, A. S. *Carbohydr. Res.* **2003**, *338*, 95–107.
32. MM3 (96). *Bull. QCPE* **1997**, *17* (1), 3.
33. Engelsen, S. B.; Koča, J.; Braccini, I.; Hervé du Penhoat, C.; Pérez, S. *Carbohydr. Res.* **1995**, *276*, 1–29.
34. Engelsen, S. B.; Rasmussen, K. *J. Carbohydr. Chem.* **1997**, *16*, 773–788.
35. Stortz, C. A. *Carbohydr. Res.* **1999**, *322*, 77–86.
36. Koča, J. *J. Mol. Struct.* **1993**, *291*, 255–269.
37. Ohanessian, J.; Longchambon, F.; Arene, F. *Acta Crystallogr. Sect. B* **1978**, *34*, 3666–3671.
38. Ikegami, M.; Sato, T.; Suzuki, K.; Noguchi, K.; Okuyama, K.; Kitamura, S.; Takeo, K.; Ohno, S. *Carbohydr. Res.* **1995**, *271*, 137–150.
39. Rao, V. S. R.; Qasba, P. K.; Balaji, P. V.; Chandrasekaran, R. *Conformation of Carbohydrates*; Harwood Academic Publishers: Amsterdam, 1998; pp 91–130.
40. Stortz, C. A. *Carbohydr. Res.* **2002**, *337*, 2311–2323.
41. Stortz, C. A.; Cerezo, A. S. *J. Carbohydr. Chem.* **2002**, *21*, 355–371.
42. Stortz, C. A.; Cerezo, A. S. *J. Carbohydr. Chem.* **2003**, *22*, 217–239.
43. Homans, S. W. *Biochemistry* **1990**, *29*, 9110–9118.
44. French, A. D.; Mouhous-Riou, N.; Pérez, S. *Carbohydr. Res.* **1993**, *247*, 51–62.
45. Imberty, A.; Pérez, S. *Carbohydr. Res.* **1988**, *181*, 41–55.
46. Jeffrey, G. A.; Huang, D.-b. *Carbohydr. Res.* **1991**, *222*, 47–55.